J. Indian Inst. Sci., 66, June 1986, pp. 411-433

IISc. THESES ABSTRACTS

Thesis Abstract (Ph.D.)

Nondeterminism and communication in functional programming systems: A study in formal program development

by Asis Kumar Goswami.
Research supervisor: L.M. Patnaik.
Department: School of Automation.

1. Introduction

Recent advancement in VLSI technology has led to the economic feasibility of building computers which are radically different from the existing ones. Future generation computers are likely to exploit the achievement in the VLSI technology by incorporating in them thousands of identical units which would function quite independently and yet cooperate on a task when necessary. Several such computers have already been built on an experimental basis. Various new language concepts have been proposed as the earlier ones were found to be incapable of utilizing the tremendous processing power of VLSI-based systems. One of these language concepts is that of Functional Programming (FP) systems[1] introduced by John Backus. FP systems are considered to have great potential for becoming the programming languages for future generation computers because they can describe highly parallel computation in a comprehensible way. Another important aspect of the FP systems which is likely to make these systems stand high in the programmers' favor is that the language used to reason about programs is essentially the programming language itself. Successful implementation of FP systems[2] and the development of simple yet powerful algebraic methods of reasoning about FP programs[3] have demostrated the feasibility of using these systems as programming languages for the next generation computers. This dissertation strengthens the power of the FP systems by presenting several results of our work on the theory and methodology of programming in certain extended and modified versions of the FP systems.

2. The proposed extensions of FP systems

There are some important aspects of programming in FP systems which have not been investigated so far. One of these is concerned with the specification of programs. The reported work on FP systems has made it possible to transform some programs into more efficient ones or to prove the equivalence of two programs. Thus the specification of a program can only be just another program. However, the use of programs as specifications does not always produce the abstraction required in many applications. Moreover, for many problems we may know only the properties of their solutions. Intuitive construction of programs from this information about problems is difficult in many cases. Hence there is a necessity for a suitable specification system and for methods of development of FP programs from their specifications. Inter-program communication and nondeterminism are

other two important aspects of programming which need attention. Interprogram communication has been found to be a useful tool for introducing parallelism into many algorithms. Several other applications such as operating systems and real-time simulation also require communication between programs. Nondeterminism is an inherent property of many problems; it has also been shown to be a useful concept by which the programmer may opt for leaving the design decisions in programs to the execution instances. In a system of communicating programs, nondeterminism in the ordering of communication contributes to the asynchrony of the programs. In this dissertation, we report the results of a fairly detailed investigation of the above mentioned aspects of programming in FP systems.

3. Main results

A set-theoretic model of nondeterminism in FP programs is developed. In the existing FP systems, programs represent functions whose arguments and images are called 'objects'. In order to introduce nondeterminism into FP systems, we have modified the functionality of FP programs; the argument and the image of an FP program are considered in this dissertation as subsets of the set of objects. This modification in the fundamental characteristic of FP programs is emphasized by naming the modified FP systems thus arrived at as 'Nondeterministic FP (NFP) systems'.

With each FP system is associated an algebra of programs; the set of programs is the carrier of the algebra. The operations of the algebra are called 'functionals'. A set of primitive programs serves as the 'generating set' of the algebra, *i.e.*, the carrier of the algebra is generated from the set of primitive programs using the operations of the algebra. A set of functional identities involving primitive programs, functionals and program variables serves as the set of axioms of the algebra so that all functional identities of the algebra can be derived from these axioms by a simple rule of substitution stating that any program variable can be replaced by an arbitrary program. Thus the algebra of programs is a powerful tool for reasoning about programs by transformations. Our modification of an FP system into an NFP system preserves the above characteristics of FP systems. Although the functionality of NFP programs is different from that of FP programs, we can show that, for each FP system, a corresponding NFP system can be designed so that a homomorphism exists from the algebra of the FP system into the algebra of the NFP system. This fact indicates that our modification of an FP system into an NFP system does not result in any loss of power of the algebra of programs. In fact, we make the algebra simpler by defining a useful FP functional 'condition'in terms of two new NFP functionals-'union' and 'restriction'. The functional union is also used to introduce nondeterminism into programs. In this dissertation, we state and justify the axioms of the algebra of programs of a typical NFP system. Just like FP systems, NFP systems also allow programs to be defined by recursive equations. In order to be able to reason about recursive NFP programs either by using known induction methods based on the fixed point theory or by the technique of program expansion developed by Backus, we describe the fixed point semantics of NFP programs. This semantics is based on the Egli-Milner ordering in the set of programs, and on the theory of complete partial orders[4].

Nondeterminism simplifies the process of program development provided that nondeterminism can be controlled by program–forming operations (functionals in FP or NFP systems). Therefore we restrict the use of the functional union and introduce nondeterminism in programs (to be executed) by a new functional – 'guarded condition', defined in terms of the functionals union and restriction. The design of the guarded condition

functional has been inspired by Dijkstra's 'guarded commands'[5] which are used to specify nondeterminism in procedural languages. As is obvious from above, we do not consider all NFP programs to be executable. We define the subset of executable programs and call these programs 'well-behaved'. Programs which are not well-behaved belong to the metalanguage used for semantic descriptions of NFP systems. A novel concept of 'regular forms' is introduced in order to put forward a disciplined way of reasoning about programs by transformations. This concept along with the use of the functional guarded condition (instead of the functional condition) is also shown to simplify the study of 'linear forms'[3], which have been proposed by Backus for the purpose of developing algebraic methods of reasoning about recursive programs. We also introduce the concept of the inverse of a program in order to analyse some properties of programs by transformations, and to enrich the transformational technique of program development. The inverse of an NFP program is again an NFP program. For the sake of notational uniformity, we consider the inverses of NFP programs to be produced by a unary functional. Yet another new functional 'intersection' is used to develop axioms (of the algebra of programs) involving inverses of programs.

In order to supplement the existing method of developmment of FP programs, we propose two approaches to the specification of programs. Choice between these approaches depends on the nature of the information available about the behavior of the program being developed. One of the specification mechanisms borrows from Backus' idea of using formal program variables for improvement in program clarity. These specifications are predicates (*i.e.*, programs having the set of boolean constants as their co-domain) involving formal input and output program variables. The specifications resemble the conventional input-output assertions[5] about programs in the procedural languages and thus are likely to be easily constructed; on the other hand, the fact that variables of our specifications represent programs makes these specifications more amenable to algebraic manipulations at the program level. The other specification mechanism describes a program by a set of 'qualified equations'[1] which, in turn, describes the functional behavior of the program in various subsets of the domain of the program. The option of using program variables and of allowing some redundancy in these specifications aids intuitive construction of these specifications. Constructive methods for development of programs from the two types of specifications are presented and supported by suitable examples.

This dissertation also includes some interesting results of our investigative work on the introduction of inter-program communication into the NFP programs and on the development of algebraic methods of specifying and reasoning about communicating programs. The communication constructs resemble, in form and in operational behavior, those of Communicating Sequential Processes[6]. An algebraic semantics of communication is also presented. A few ideas on reasoning about communicating NFP programs and on the specification and formal development of these programs are proposed and illustrated by examples. We show that it is very convenient to reason about terminating communicating programs by translating these programs (using the axioms of communication) into noncommunicating ones. Even for nonterminating communicating programs, the verification and development processes involve only the analysis of the intermediate objects produced by the noncommunicating versions of these programs. The fact that the communicating NFP programs are 'communication-closed layers'[7], makes these programs amenable to very simple and elegant mathematical analysis.

References

1. BACKUS, J. — Can programming be liberated from the von Neumann style? A functional style and its algebra of programs, *Comm. ACM*, Aug.1978, **21**, 613-641.
2. MAG'O, G. — A cellular computer architecture for functional programming. Conf.Record COMPCON SPRING, 1980, pp.179-187.
3. BACKUS, J. — The algebra of functional programs: Function level reasoning, linear equations, and extended definitions, *Lecture notes in computer science*, 107, Springer-Verlag, Berlin, 1981, pp.1-43.
4. DE BAKKER, M. — Mathematical theory of program correctness, Prentice-Hall, New Jersey, 1980.
5. DIJKSTRA, E. W. — A discipline of programming, Prentice-Hall, New Jersey, 1976.
6. HOARE, C. A. R. — Communicating sequential processes, *Comm.ACM*, Aug.1978, **21**, 666-677.
7. ELRAD, T. AND FRANCEZ, N. — Decomposition of distributed programs into communication-closed layers, *Sci. Computer Programming*, 1982, **2**, 155-173.

Thesis Abstract (Ph.D.)

Feeding of permanent moulded spheroidal graphite iron castings by M.S. Chandrasekhara Rao.
Research supervisor: Malur N. Srinivasan.
Department: Mechanical Engineering.

1. Introduction

This thesis deals with the problem of feeder dimensioning of permanent moulded spheroidal graphite iron castings. Detailed studies have been made not only on the effectiveness of feeders in eliminating internal porosity, but upon the influence on structure and mechanical properties during this course.

It has been demonstrated earlier[1] that feed metal requirements for permanent moulded spheroidal graphite iron castings can be kept to a minimum by having more than three per cent silicon in the castings. But such castings are susceptible to low fracture toughness at ambient temperature[2]. Thus to have good fracture toughness at ambient temperature it would be desirable to have lower levels of silicon in the castings. But there would be concomitant increase in the chilling tendency and consequent increase in feed metal requirements. The latter cannot be assessed from feeding equations applicable to sand castings in view of differences in the mode of solidification. A survey of literature indicated that there is very little information on feeder dimensioning of permanent moulded spheroidal graphite iron castings. The present investigation was taken up with this in view.

Feeder dimensions have been determined for uninoculated castings, as inoculation would tend to offset to some extent the objective of maintaining low levels of silicon in the castings. However, it has also been established in the present work that inoculation reduces the feeding requirements, implying that the feeder dimensions determined provide conservative estimates of those required for inoculated castings. Detailed studies have also been made on the microstructure and mechanical properties of the castings as influenced by feeders.

2. Experimental programme

2.1. Test casting

The test castings chosen were plates of varying thickness cast vertically. The feeders used were of trapezoidal shape of varying heights. Plate castings were individually cast initially and solidification time of each casting was determined at initial mould temperatures of 200° and 300°C. Likewise the solidification times of corresponding feeders of different heights were determined when individually cast at 200°, 300° and 400°C initial mould temperatures. Subsequently all the different casting-feeder combinations were poured and the microstructures, density and mechanical properties of all the castings were determined after subjecting the castings to a standard heat treatment.

2.2. Alloy composition, melting and pouring

Low silicon base iron (2% Si) of near eutectic composition (C.E.=4.2) was used. The alloy was melted in a direct arc electric furnace lined with high alumina air setting refractory cement. Sandwich method was adopted for nodularising the molten metal with one per cent nickel-magnesium alloy. The molten metal was tapped at a temperature of 1450°C and the treated molten metal was poured into the coated moulds at a temperature of about 1350°C.

2.3. Heat treatment

Castings were stripped from the moulds after cooling them to room temperature and were subjected to standard heat treatment by heating to 910°C and holding at this temperature for eight hours, followed by furnace cooling. For density measurement the samples were given an additional (ferritizing) heat treatment.

2.4 Test on castings

Radiographic examination (to assess soundness of castings), density measurement, microstructural analysis and mechanical tests were conducted on each casting after the standard heat treatment.

2.5. Statistical design of experiments

Statistically designed experiments were conducted to study the effect of inoculation on microstructure, volume deficit and mechanical properties of the castings using factorial 2^3 experiments. The three independent variables chosen were inoculation percentage, mould preheating temperature and casting thickness.

The same melting procedure was adopted as outlined in section *2.2.* In addition, post-inoculation was made to the molten metal soon after the nodularising reaction had

subsided in the crucible. The inoculant used was foundry grade ferro-silicon having 75% silicon. The provision of an overflow core ensured that each mould was filled to the same extent with the molten metal. The same procedure of heat treatment and tests on castings was adopted, as explained in sections *2.3* and *2.4*.

3. Conclusions

3.1. Based on the systematic analysis of the data obtained to assess the dimensions of the feeders for permanent moulded spheroidal graphite iron castings the following conclusions can be drawn.

3.1.1. The solidification time (τ in seconds) of individually cast plate castings and trapezoidal feeders can be related to the respective volume to surface area ratio (V/SA in mm), by a relationship of the type $\tau = K(V/SA)^n$, where K and n are positive constants.

3.1.2. The solidification times of both individually cast plates and trapezoidal feeders increase with the initial mould temperature.

3.1.3. From the plot of solidification time ratio *vs* volume ratio (fig.1), following feeding equation is obtained,

$$^{\tau}R/^{\tau}C = \frac{0.77}{V_R/V_C - 0.006} + 1.0$$

where the subscripts *C* and *R* refer to the casting and the feeder respectively. Feeder nomograms have been constructed based on the above feeder equation.

3.1.4. The density of the specimens taken at the mid-region of the castings tends to decrease at high values of the solidification time ratio.

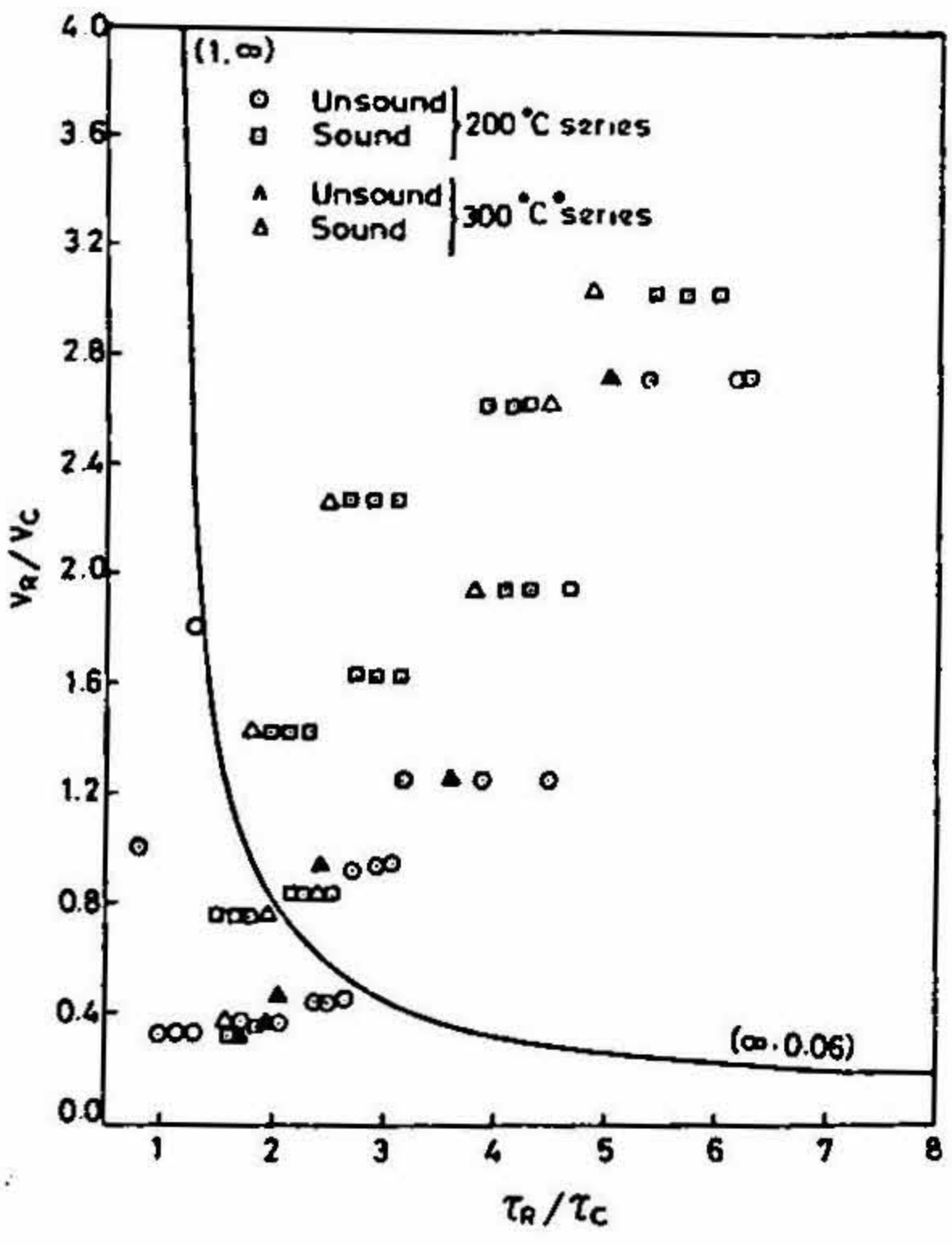

FIG.1. Plot of solidification time ratio *vs* volume ratio.

3.1.5. There is appreciable scatter in the relationship between graphite particle count or ultimate tensile strength or elongation and the solidification time ratio.

3.1.6. There appears to be no simple relationship between the microstructural details as represented by the graphite morphology and the matrix features and the cooling rate variable studied in the series.

3.1.7. Good mechanical properties in this series are obtained when the density of the casting is high and when the microstructure consists of well-developed nodules distributed in a ferritic matrix.

3.2. From the statistically designed experiments conducted to study the effect of simultaneous variation of inoculant, casting size and initial mould wall temperature on the volume deficit, microstructure and mechanical properties it is observed:

3.2.1. Simultaneous increase in inoculant percentage, casting thickness and initial mould wall temperature tend to minimise the external volume deficit leading to dimensionally more accurate castings.

3.2.2. The effectiveness of inoculation in reducing the external volume deficit is better at high or low cooling rates than at intermediate cooling rates.

3.2.3. Inoculation is more effective in increasing the nodule count of thinner castings.

3.2.4. Inoculation improves the distribution of nodules provided the cooling rates are relatively low.

3.2.5. The matrix obtained following the standard heat treatment is predominantly ferritic in all the inoculated castings.

3.3 It is clear that uninoculated permanent moulded spheroidal graphite iron castings of acceptable internal soundness can be produced when feeder dimensions are determined from the feeder equation obtained in the present investigation. However the mechanical properties of these castings vary in a way which cannot be easily predicted owing to microstructural variations. Consistency in the latter can be significantly improved by adequately post-inoculating with ferro-silicon.

References

1. NARENDRANATH, C.S. *Studies on permanent moulded magnesium treated cast iron,* Ph.D. Thesis, Indian Institute of Science, Bangalore, 1982.

2. SEETHARAMU, S. *Fracture toughness of permanent moulded magnesium treated iron castings,* Ph.D. Thesis, Indian Institute of Science, Bangalore, 1981.

Thesis Abstract (Ph.D.)

Role of ozone in sun-weather relationships by M. Giridhar Krishna.
Research supervisors: S. Ramakrishna and N. Balakrishnan.
Department: Aerospace Engineering.

1. Introduction

A number of mechanisms have been proposed to account for the influence of solar activity on weather. Some of the mechanisms proposed take into consideration the possible influence of solar activity on stratospheric ozone. These mechanisms include the solar cycle modulation of atmospheric ozone and the planetary wave mechanism[1] and they have been critically examined in the present work.

2. Solar cycle modulation of atmospheric ozone

It has been suggested that the production of ozone should vary with the solar cycle[1]. Accordingly, maximum ozone is expected to occur in the sunspot maximum year and minimum ozone in the sunspot minimum year. Based on this assumption it is felt that the ozone layer would produce a 11-year period modulation in the amount of solar ultra-violet (UV) radiation reaching the lower atmosphere. This is expected to induce a similar modulation on the global annual average temperature.

To examine this mechanism, the relationship between solar/geomagnetic activity and total atmospheric ozone during the sunspot minimum year 1976 and the sunspot maximum year 1979 has been studied at five selected stations–Resolute, Churchill, Hohenpeissenberg, Wallops Island and New Delhi. The solar activity indices used are the daily relative sunspot number (R_z) and the solar 10.7 cm radio flux ($F_{10.7}$) and the geomagnetic index used is the A_p index.

A study of the photochemistry of ozone reveals that solar activity can have both short term as well as long term influences on atmospheric ozone. To distinguish between these influences a rank deviation technique which separates the ozone data into two groups has been developed. The two groups have then been individually correlated with the solar and geomagnetic activity indices.

The analysis with R_z and $F_{10.7}$ shows that the relationship between solar activity and atmospheric ozone undergoes significant changes between the sunspot minimum and maximum years. The correlations remain positive in 1976 (sunspot minimum year), while nearly 50% of the days show negative correlation in the sunspot maximum year 1979 (Table I). These changes can be attributed to the more frequent occurrence of solar proton events and relativistic electron precipitation events around the sunspot maximum[2,3]. This leads to depletion of ozone, tending to offset any enhancement in ozone due to increased solar UV radiation. The analysis with the geomagnetic activity index A_p reveals low correlations in both 1976 and 1979. However, a superposed epoch analysis shows a significant depletion of ozone, especially at higher latitude stations, 9–10 days after the occurrence of geomagnetic disturbances caused by solar flares. The observed change in the relationship between solar activity and atmospheric ozone with the solar cycle seems to indicate that a solar cycle modulation of atmospheric ozone may not occur. Hence, it may be an unlikely mechanism for sun-weather relationships.

Table I
Correlations for total ozone and sunspot–1972

Station	No. of days of data	No. of days in two groups	Correlation coefficient*	Lag
Resolute	240	122	0.45	0
		118	−0.66	3
Churchill	349	166	0.50	0
		183	−0.62	1
Hohenpeiss-enberg	236	119	0.42	0
		117	−0.68	0
Wallops Island	280	158	0.38	0
		122	−0.74	0
New Delhi	332	172	0.51	0
		170	−0.71	0

*All correlations significant at the 0.00001% level.

3. Planetary wave mechanism for sun-weather relationships

Tropospheric planetary waves which propagate upwards into the stratosphere and transfer heat polewards can influence the longitudinal variations of surface climate[4]. Changes in the stratospheric structure are likely to modify the altitude and degree of down reflection of the planetary waves. These changes in the characteristics of the planetary waves may affect the surface climate[5]. Since stratospheric structure is determined by the wind, temperature and ozone in the stratosphere, any influence of solar activity on these stratospheric parameters will affect the planetary waves and hence the surface climate. It may be mentioned here that planetary waves can penetrate only the winter stratosphere. Hence a study of the relationship between solar activity and atmospheric ozone in the winter months November-February during the period 1976–1979 has been carried out at the five stations being considered here.

The analysis for the winter months shows that nearly 30% of the days show a negative correlation with R_z and $F_{10.7}$ in the sunspot minimum year at all the five stations. In the years around the sunspot maximum very few days show a negative correlation whereas significant positive correlations are observed between ozone and both the solar activity indices (Table II). These results are quite different from those obtained when the entire year's data was considered. This difference can be attributed to increased planetary wave activity in the sunspot maximum year which leads to large-scale transport of ozone from the lower latitudes to the higher latitudes thus masking any depletion in ozone due to solar proton events. A relationship between solar activity and planetary wave activity is therefore indicated by these results. To establish such a relationship a study has been carried out on the influence of solar activity on stratospheric warmings which occur in the winter stratosphere due to the upward propagation of planetary waves. The study reveals that major warmings tend to begin 2–5 days before a peak in sunspot number (fig. 1). The rise in temperature during a stratospheric warming also seems to be significantly larger around a sunspot maximum year. These observations along with the results obtained for the winter analysis of data seem to indicate that a relationship between solar activity and planetary wave activity is a definite possibility. Thus the planetary wave mechanism seems to be a more likely candidate for sun-weather relationships.

Table II
Total ozone-R_z correlations at Churchill in winter

Period	No. of days of data	No. of days in two groups	Correlation coefficient	Lag	Significance %
1975–76	115	72	0.52	0	0.00005
		43	−0.64	2	0.0001
1976–77	118	103	0.44	0	0.00001
		15	−0.87	0	0.001
1977–78	117	86	0.48	0	0.001
		31	0.64	15	0.0025
1978–79	118	105	0.55	0	0.00001
		13	0.89	15	0.00025

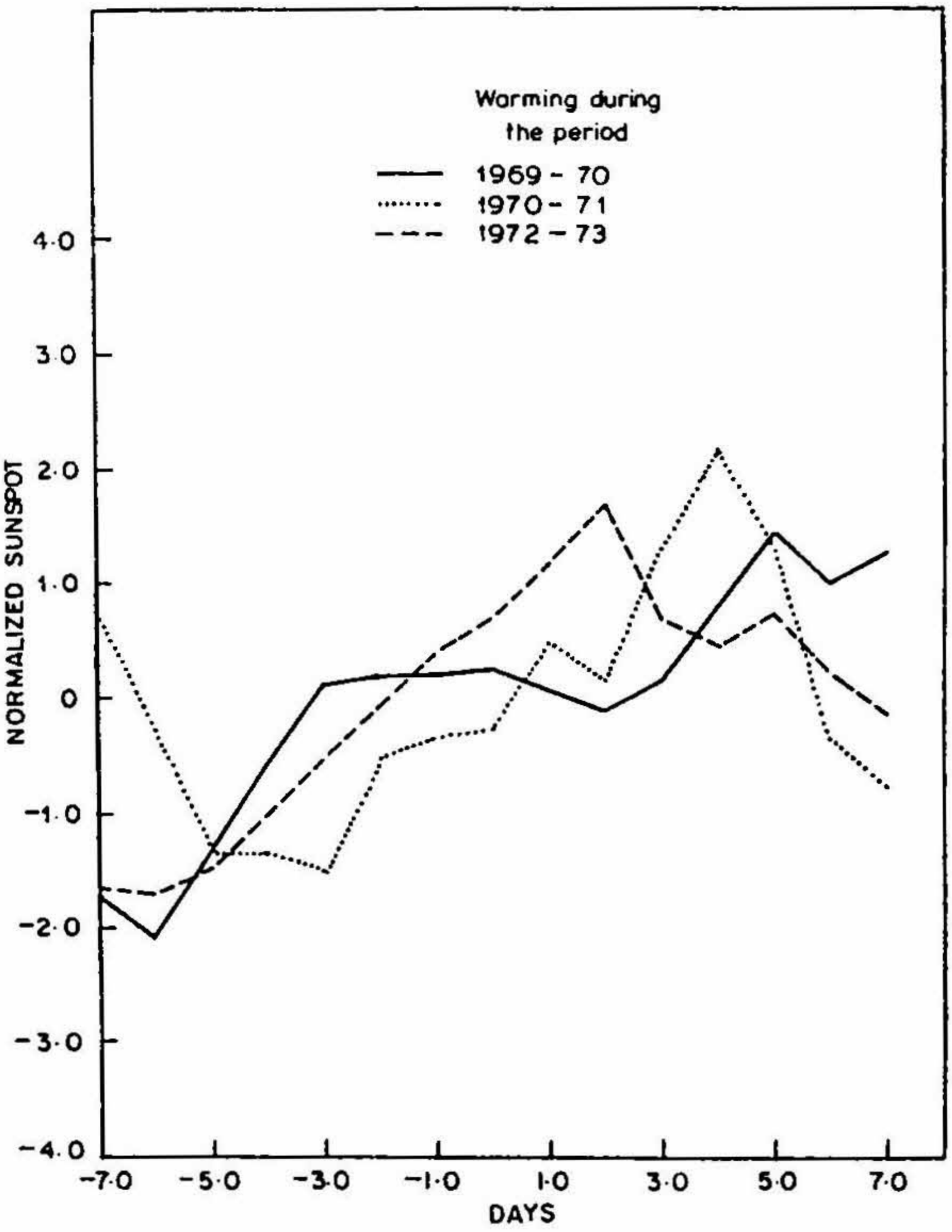

FIG 1. Variation of sunspot around stratospheric warming begin date.

References

1. HERMAN, J.R. AND GOLDBERG R.A. *Sun, weather and climate*, NASA SP-426, 1978.
2. HILL, G.E. Synoptic charts of F_{min} in *Research concerning forecasting anomalous propagation at high latitudes*, AFCRL-63–54, 1963.
3. THORNE, R.M. A possible cause of dayside relativistic electron precipitation events, *J. Atmos. Terr. Phys.*, 1974, 635–645.
4. Middle atmospheric program planning, Document prepared at the MAP planning conference, 1976, p. 12.
5. BATES, J.R. A dynamical mechanism through which variations in solar UV radiation can influence tropospheric climate, *Solar Phys.*, 1981, **74**, 399–415.

Thesis Abstract (Ph.D.)

Studies on compacted graphite cast irons by V. Sri Ramachandra Murthy.
Research supervisors: S. Seshan and Kishore.
Department: Mechanical Engineering.

1. Introduction

Compacted graphite cast iron (CG iron) is a recent addition to the family of cast irons. This new material is also popularly known as 'Vermicular graphite cast iron' (VG iron). CG iron was an accidental outcome during the large tonnage production of ductile iron castings and was initially considered as a degraded form of iron. But the recent developments in processing controls and materials have made the international production of CG irons attractive.

2. Materials and methods

In this investigation, CG irons have been produced repetitively and consistently using three methods *viz.*, (a) Under-treatment with spheroidizing material (Mg), (b) combined treatment with spheroidizing and anti-spheroidizing elements (Mg, Ti and Al), and (c) treatment of low-sulphur pig iron with zirconium (to obtain coral graphite). Of all the methods, combined treatment with spheroidizing and anti-spheroidizing materials has been found to be the most effective and flexible. Production of CG iron in permanent moulds was also accomplished through the combined treatment by altering the proportion of spheroidizing and anti-spheroidizing materials. Test pieces taken from sand cast blocks were subjected to thermal treatment with a view to alter the matrix structure. In subsequent studies, CG iron was alloyed with copper and nickel; the combined addition of copper and nickel resulted in as-cast bainitic structures in thin sections.

In CG irons the graphite is present in stubby, worm-like form with rounded edges. Compacted graphite in sand-cast CG iron has been found to be uniformly distributed

whereas in permanent moulded CG irons, graphite compacts are present as well-distributed clusters.

During solidification CG iron shows undercooling, the degree of which is in between gray and ductile irons. The eutectic cell size in the case of CG irons is larger than ductile irons. Compacted graphite iron has interconnected graphite in the form of three-dimensional network even though it appears isolated in two-dimensional structure. Unlike flake graphite, the ends of compacted graphite are more ronud and blunt (fig.1). The growth of these graphites was observed to be in spiral form. It appears that the formation of compacted graphite is possibly mainly by two methods *viz.*, degeneration of spheroids or explosion of spheroids. The growth of compacted graphite seems to be predominantly in C-axis direction of hexagonal graphite crystals (whereas, flake and spheroidal graphites grow in A and C directions respectively). Based on the observations, a new growth model has been proposed in this investigation.

It has been found that section sensitivity of CG irons is dependent on chemical composition; at eutectic composition CG iron is very section-sensitive. The fluidity of CG irons is akin to the fluidity of gray irons rather than ductile irons. Solidification shrinkage of CG irons varies from 2 to 3%. In general, the mechanical properties CG irons have been found to be intermediate between those of gray and ductile irons. Even in the as-cast condition, ultimate tensile strength of CG iron is superior to that of gray iron, and a measurable elongation is noticed (fig.2). The effect of aspect ratio of graphite has been assessed and relationships obtained between the aspect ratio and mechanical properties. The effect of chemical composition on mechanical properties was found to be negligible. For a given aspect ratio of graphite, properties could be improved by altering the matrix structure through thermal treatment or by alloying. As-cast bainitic CG irons exhibit the highest strength among the alloyed irons. Failure analysis was carried out on tensile,

FIG 1. Blunting and rounding of edges of compacted graphite.

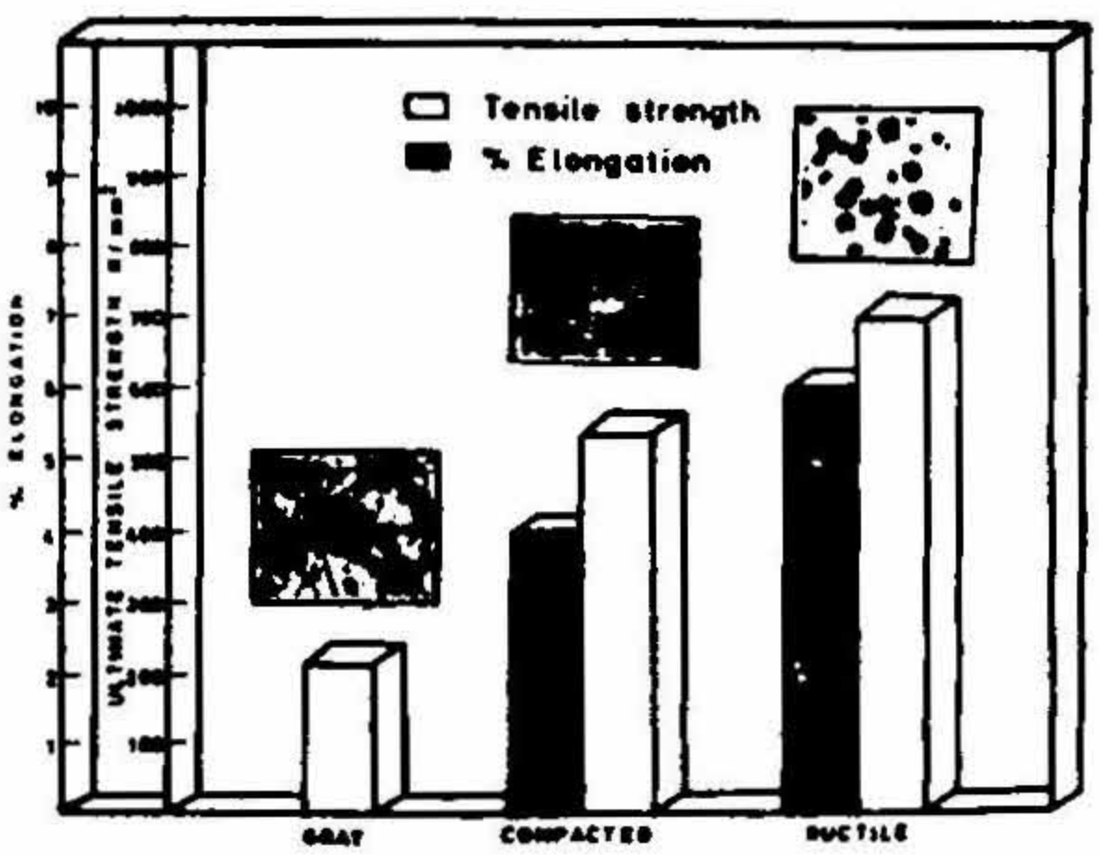

FIG 2. Tensile properties of gray, compacted and ductile irons.

impact and fatigue samples. The analysis of test samples showed partly brittle failure features of gray iron and partly of ductile iron.

Wear properties of CG irons have been assessed and the superior wear properties of these irons have been justified based on the mechanical properties, graphite film formation and the mechanisms operating in the process of wear. The wear properties have also been found to get improved, in general, by conventional heat treatment and by alloying. Delamination process of wear seems to be operating in all the cases. To explain the complex wear process, a new factor called 'wear resistance factor' has been introduced in this work. Machinability of CG irons has been found to be good, and the weldability is satisfactory. Corrosion resistance of CG irons, which is already superior to ductile irons, could be further improved by the addition of copper and nickel. Oxidation behaviour at higher temperatures is satisfactory.

3. Conclusion

Probable applications for CG irons have been suggested. Taking into account the cost of raw materials and power, a cost-analysis for the production of gray, CG and ductile irons has been attempted.

References

1. SISSENER, J.,. THURY, W., HUMMER, R. AND NECHTELBERGER, E. — Cast iron with vermicular graphite, *Inter. Cast Metal J.*, 1972, **8**(4), 178–181.
2. MURTHY, V.S.R. KISHORE AND SESHAN, S. — Properties of cast iron with compacted graphite, *Br. Foundryman*, 1985, **78**(2), 71–77.
3. MURTHY, V.S.R., SESHAN, S, AND KISHORE — Wear behaviour of compacted graphite cast iron investigated, *Foundry Trade J.*, 1985, **159** (No. 3311), 132–134, 140.
4. MURTHY, V.S.R., KISHORE AND SESHAN, S. — Characteristics of compacted graphite cast irons, *Trans. Am. Foundrymen's Soc.*, 1984, **92**, 373–379.

Thesis Abstract (M.Sc.Engng.)

Multiprocessing architecture for parallel hidden surface removal algorithm

by Dipak Ghosal.
Research supervisor: L.M. Patnaik.
Department: School of Automation.

1. Introduction

With the advent of powerful and inexpensive VLSI devices, interactive computer graphics has attained a great deal of significance and wide applicability. The utility of interactive

computer graphics has been established in a multitude of areas such as interactive plotting in business and scientific applications, cartography, CAD/CAM, simulation, animation, process control, office automation, entertainment, to name only a few. The list of applications continues to grow rapidly as simple display systems become routinely affordable due to declining hardware costs.

One of the exciting and potentially important areas in interactive computer graphics is the synthetic generation of realistic images depicting modeled solid objects. Applications of solid modeling include CAD/CAM, architectural construction, molecular modeling and many others. The main problem limiting the use of solid modeling has been the excessive time required to generate images corresponding to new viewpoints. The identification and removal of hidden surfaces have been a major area of research in interactive computer graphics. The hidden surface removal algorithms[1] are required to perform enormous amount of computation even for objects of moderate complexity. This renders a computer graphics system useless in many 3D applications, requiring fast interaction particularly in real-time environments. Many schemes have been studied for increasing the computational efficiency of the hidden surface removal algorithms. These include more efficient data representation methods[2] and parallel processing[3,4] techniques. In this thesis, parallel processing techniques have been studied to speed up the hidden surface removal process.

2. Overview of the work

The work reported in this thesis is primarily concerned with the design and performance evaluation of hidden surface removal algorithms to be executed on multiprocessing systems. The parallel hidden surface removal algorithms designed use parallel sorting techniques and exploit coherence[5] inherent in the objects to be displayed. Three hidden surface removal algorithms have been considered and their modified parallel versions are presented in this dissertation. The performance of these algorithms has been evaluated using SIMPAR: a *SI*mulator for *M*ultiprocessing *AR*chitectures. SHAMP: a *SH*ared *M*emory multi*P*rocessing system has been implemented using five Intel's single board computers to carry out experimental studies of the parallel architecture. SHAMP has enabled us to validate the simulation strategy adopted in the design of SIMPAR. It has also provided hands-on experience in both the software and hardware aspects of the design of multiprocessing systems for hidden surface removal problems.

3. Parallel algorithms for hidden surface removal

The three hidden surface removal algorithms considered in this dissertation are the depth sort algorithm, the scan line algorithm, and the Warnock's area subdivision algorithm. It has been shown that polygon scan conversion is an underlying feature in most hidden surface removal algorithms and this is especially true for the three hidden surface removal algorithms considered in this thesis. Hence systematic development of an efficient hidden surface removal algorithm purports to the design of an efficient parallel polygon scan conversion algorithm. In this work, three different parallel polygon scan conversion algorithms PA1, PA2 and PA3 have been proposed. These algorithms differ in the extent to which they exploit coherence inherent in the polygon to be displayed. Theoretical speed-up factors for these algorithms have been calculated based on simple analytical methods[6]. The parallel depth sort algorithm and parallel scan line algorithm have been proposed and these have been shown to follow directly from the parallel polygon scan conversion algorithms.

The Warnock's area subdivision algorithm for hidden surface removal is, however, different from the other hidden surface removal algorithms as it uses a divide and conquer strategy. A similarity has been observed between the Warnock's algorithm and the quicksort algorithm and this greatly helps in developing an efficient, modified quicksort algorithm. Such a similarity is reflected in the modified Warnock's algorithm proposed in this work.

3.1 Similator design

SIMPAR: a *SI*mulator for *M*ulti*P*rocessing *AR*chitectures is a software module which simulates a shared bus multiprocessing system on which parallel algorithms can be executed to measure their performance. The basic design methodology adopted in modeling concurrent processes on a uniprocessor system has been employed in the construction of the simulator. By varying the number of processors of the simulated multiprocessing system, the user can obtain various performance measures as a function of the number of processors. SIMPAR provides an excellent tool for performance evaluation of parallel algorithms to be executed on a multiprocessing system.

3.2. Experimental hardware system

SHAMP: a *SHA*red *M*emory multi*P*rocessing system is the experimental system built using five Processing Elements (PEs) based on Intel's family of microprocessors and peripherals. These PEs are connected to a global shared memory *via* a common bus. The system has two Intel iSBC 86/30[7] and three Intel iSBC 86/12A[8] boards each of which contains 16–bit processing units (Intel 8086), local dual port memory and some I/O interfaces. The common bus is an Intel Multibus equipped with a specially constructed bus arbiter. The global shared memory is an Intel iSBC 028A memory card containing 128K bytes of RAM which can be accessed *via* the Multibus. The system is interfaced with an Intel Series III Microprocessor Development System which also acts as the sole I/O device for SHAMP. The processors, the global memory and the arbiter board are mounted on a specially constructed chasis. All the relevant software has been developed in PL/M 86.

4. Results

The following are the important results obtained through simulation, theoretical and experimental studies reported in the thesis. (i) The results obtained from the simulation and experimental studies have been compared to validate the strategy adopted in the design of SIMPAR. The performance factors obtained for the various algorithms from the analytical method, simulation and experimental studies shown an excellent agreement. (ii) The performances of the three parallel polygon scan conversion algorithms have been compared to study the relative merits of the three algorithms when executed on a shared bus architecture. (iii) It has been shown through simulation and experimental results that the execution of parallel polygon scan conversion algorithms on a shared bus architecture does not result in a high Processing Power* for a large number of processors. This significant degradation in performance is due to the inherent coherence present in the algorithm which causes a high bus contention. This observation helps in proposing a

* Processing Power is the sum of the utilization factors of the individual processors.

modified multiprocessing architecture for hidden surface removal algorithms. This modified architecture has been shown to perform better than a shared-bus architecture. (iv) The performance of the parallel depth-sort algorithm and the parallel scan-line algorithm for hidden surface removal has been presented. (v) The performance of the parallel modified quicksort algorithm when executed on a shared-bus multiprocessing architecture is also analysed in the thesis. (vi) Performance of the shared-bus multiprocessing architecture obtained from the simulation studies has been compared with that obtained from the analytical models[9] reported in the literature.

The various results show that the hidden surface removal process can be substantially speeded up using parallel processing techniques. In the case of sequential hidden surface removal algorithms, use of coherence always results in computationally efficient algorithms. This, however, is not the case in the parallel version of these algorithms. In the parallel algorithms, use of coherence may result in 'loss of parallelism' thereby exhibiting inferior performance.

References

1. FOLEY, J. D. AND VAN DAM, A. — *Fundamentals of interactive computer graphics*, 1982, Addison-Wesley Pub. Co., Reading.
2. DOCTOR, L. J. AND TORBERG, J. G. — Display techniques for octree encoded objects, *IEEE Computer Graphics Applic.*, 1981, **1**(3), 29–38.
3. BAER, J. L. — Multiprocessing systems, *IEEE Trans. Computers*, 1976, **C-25** (12), 1271–1277.
4. HWANG, K. AND BRIGGS, F. E. — *Computer architecture and parallel processing*, 1984, Mc-Graw Hill, Inc.
5. SUTHERLAND, I. E. SPROUL, R. F. AND SCHUMACKER, R. A. — A characterization of ten hidden surface removal algorithms, *Computing surv.*, 1974, **6**(1), 1–51.
6. PARZEN, E. — *Modern probability theory and its applications*, 1960, John Wiley & Sons, New York.
7. — *Intel iSBC 86/30 single board computer hardware reference manual*, Order No. 144044–001, 1982, Intel Corp.
8. — *Intel iSBC 86/12A single board computer hardware reference manual*, Order No. 9803074, 1978, Intel Corp.
9. MARSAN, A. M. BALBO, G. AND CONTE, G. — Comparative performance analysis of single bus multiprocessor architecture, *IEEE Trans. Computers*, 1982, **C-31**(12), 1185–1191.

Thesis Abstract (Ph.D)

Electrochemical aspects of sulphide mineral dissolution by M.K. Yelloji Rao.
Research supervisor: K.A. Natarajan.
Department: Metallurgy.

1. Introduction

Multimetal sulphides containing copper-zinc-lead and copper-nickel-molybdenum invariably associated with iron sulphides occur in different parts of India. Studies on the

synthesis, structure and mechanisms of different sulphide mineral reactions have been discussed in the literature[1]. Also, some studies have been made to understand the electrochemical behaviour of some sulphide minerals with respect to the various components present and their specialized electronic properties[2]. Practical problems are associated with both the mineral beneficiation as well as the extraction procedures used in the processing of these complex sulphides. It is also reported[3] that it is easier and more economical to produce initial bulk concentrates and then selectively leach the desired mineral or minerals. However, before developing any such leaching procedure, it is essential to have a basic understanding of the dissolution characteristics of the various minerals present in the ore body. The present work was undertaken in this context.

The main obectives of this work are:

i. Establishment of the fundamental electrochemical characteristics of individual sulphide minerals and their various binary combinations.

ii. Demonstration of the utility of Eh-pH diagrams in the hydrometallurgical processing of complex sulphide minerals.

iii. Development of an electrochemical procedure for the selective leaching of complex concentrate mixtures.

2. Experimental programme

The fundamental electrochemical behaviour of various sulphide minerals, pure sulphide mineral slurries and of some flotation concentrates have been studied. Under open circuit conditions, individual electrode potentials as a function of pH and aeration, combination potentials and galvanic currents have been measured whereas galvanic interaction effects for various bimineral combinations have been studied through Scanning Electron Microscope (SEM). Studies under both static and polarization studies have been made as a function of both aeration and acid concentration (sulphuric acid).

The selective dissolution of an active sulphide by galvanic contact with a nobler sulphide was studied and then compared with its selective dissolution under a desired applied potential. Effect of pH, pulp density and duration of leaching have also been studied. All the studies were conducted in sulphuric acid of required concentration. Models to explain the role of galvanic interaction, oxidative and non-oxidative dissolution in mixed sulphides have been presented.

3. Main results and conclusions

The measured redox potential values for the various sulphide minerals as a function of pH (Eh–pH) were found to be different from those predicted by theory due to the following possible reasons.

i)Presence of impurities in the system
ii)Formation of surface films at the electrode surface.

At all alkaline pH-levels, all sulphide minerals appear to follow an empirical formula $E = E' - 0{\cdot}059$ pH similar to the one put forward for a platinum electrode[4]; where E′ usually assumes a value between 0·8 and 0·9 V. In the acidic pH ranges, the measured potentials for the various sulphide minerals exhibit random scattering over a wide potential range which may correspond to an active (corrosion) region.

Table I
Individual electrode potentials, combinations and galvanic currents for the combination

Cathode (S_1)	Anode (S_2)	Electrode potentials before contact, mV *vs* SHE		E_{comb} mV *vs* SHE	i_{gal} μA
		S_1	S_2		
Pyrite	Molybdenite	505	335	412	−2·0
Pyrite	Chalcopyrite	505	400	438	−18·0
Pyrite	Pyrrhotite	505	355	418	−23·0
Pyrite	Galena	505	295	415	−22·0
Molybdenite	Chalcopyrite	335	410	375	+18·0
Molybdenite	Pyrrhotite	335	357	343	+22·5
Molybdenite	Galena	335	295	315	−23·0
Chalcopyrite	Pyrrhotite	400	355	375	−3·0
Chalcopyrite	Galena	400	295	355	−7·5
Pyrrhotite	Galena	355	295	320	−4·5

The measured individual and combination potentials along with the galvanic currents are given in Table I. An arrangement of individual electrode potentials (electrochemical activity) in their increasing order in a sulphuric acid medium of pH 2·5 in the presence of oxygen is represented below as a galvanic series.

Pyrite
Molybdenite
Chalcopyrite
Sphalerite
Pyrrhotite
Galena

↓ Increasing activity

The combination potentials were found to assume a value in between the individual electrode potentials. The magnitude and sign of the galvanic current measured in different sulphide mineral couples are dependent on the potential difference between the anode and the cathode. Large galvanic currents were observed in couples containing two minerals which are further apart in the galvanic series.

Possible surface reactions due to galvanic interaction could be explained on the basis of combination potentials and the theoretical Eh-pH diagrams. Figure 1 shows a scanning electron micrograph of the corroded surface of sphalerite after it was in contact with calcopyrite.

The anodic corrosion of an active sulphide due to galvanic interaction effect could be made use of in its selective dissolution. A lesser surface area ratio between anode and cathode, longer duration of contact and the presence of oxygen are the factors which are favourable for increased selective dissolution. For a sphalerite-chalcopyrite concentrate mixture, all the above parameters were found to be valid. A model for such a galvanic interaction is given in fig 2, along with the anodic and cathodic reactions.

Through polarization studies, the equilibrium current density, working potential range as well as the Tafel slopes for both cathodic and anodic curves have been calculated as a function of aeration conditions and acid concentration. The equilibrium current density was obtained for the condition when the rate of the anodic and cathodic processes became equal.

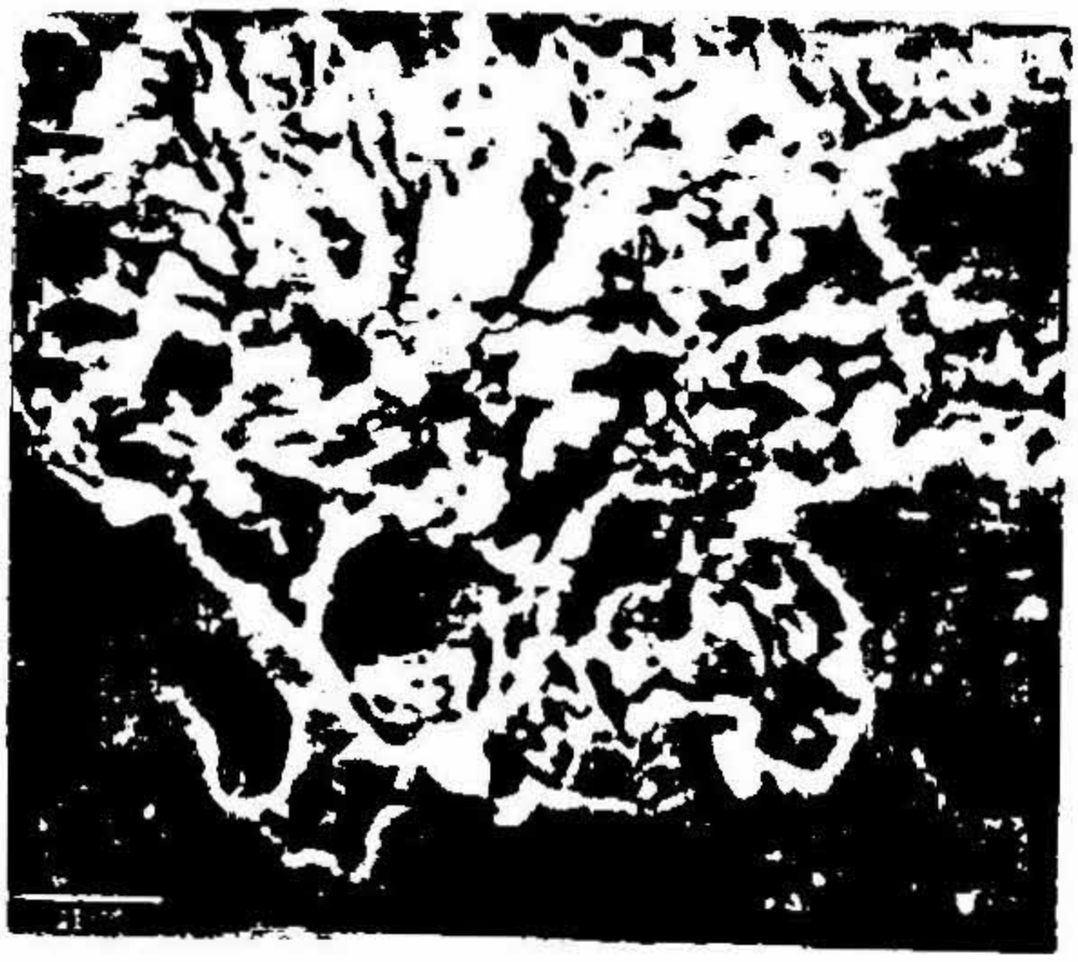

FIG 1. Scanning electron micrograph of sphalerite surface after contact with chalcopyrite.

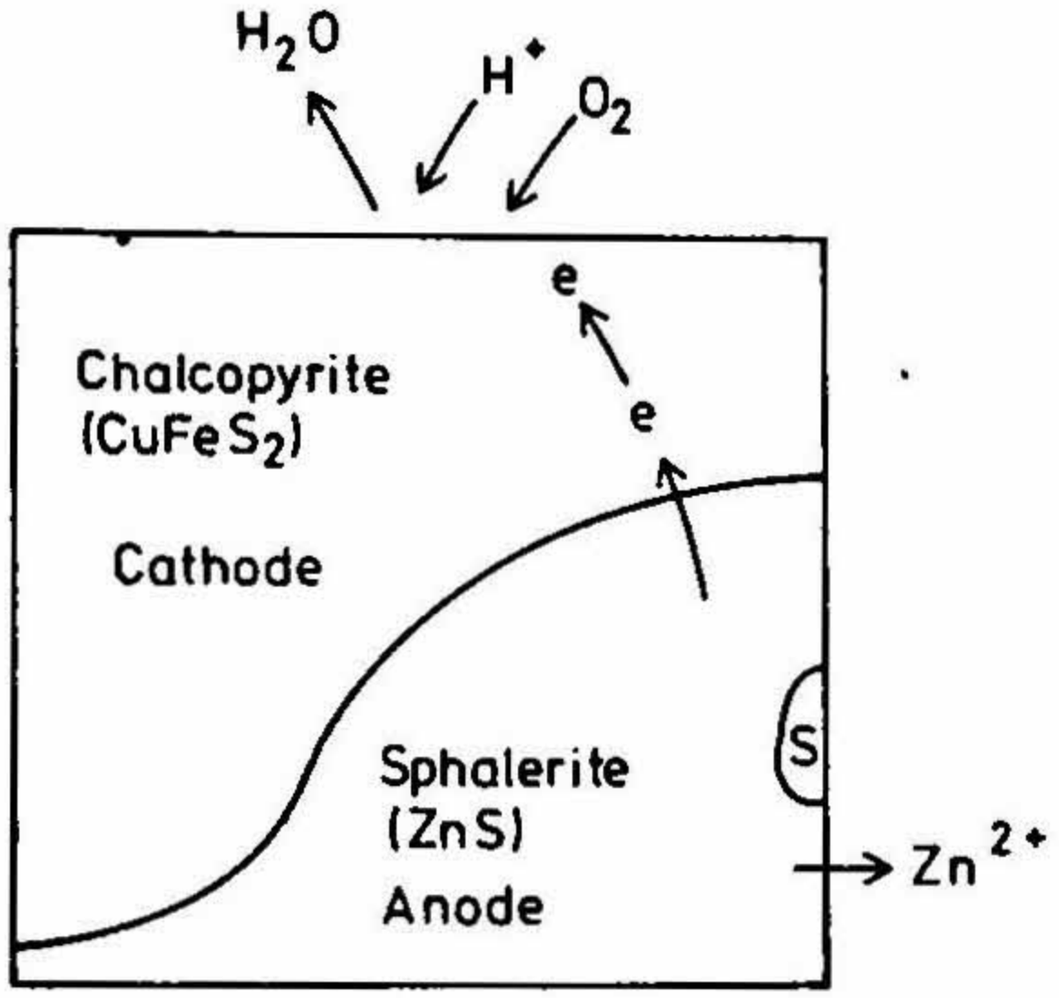

FIG 2. A model showing galvanic interaction mechanism for the sphalerite-chalcopyrite combination.

Anodic reaction: $ZnS \rightarrow Zn^{2+} + S + Ze$
Cathodic reaction: $O_2 + 4H^+ + 4e \rightarrow ZH_O$
(Oxygen reduction on cathodic surface)

Zinc can be selectively dissolved from a sphalerite-chalcopyrite concentrate mixture at an applied potential of –0·4 V *vs* Saturated Calomel Electrode (SCE). A decrease in the dissolution rate was found when the pH was increased. An optimum pulp density has to be used for better selective zinc dissolution as the relationship between pulp density and amount of zinc dissolved was found to be non-linear. The copper and zinc dissolution rates were found to be higher in the initial stages, decreasing with further increase in time. Comparison of anodic (zinc) dissolution under galvanic interaction and under applied potential conditions from a sphalerite-chalcopyrite concentrate mixture indicate that the latter technique is more advantageous.

References

1. KOCH, S.F.A. In *Electrochemistry of sulphide minerals. Modern aspects of Electricity* edited by J.O'M. Bockris and B.E. Conway, Plenum Press, New York, 1975, **10**, p. 211.

2. PETERS, E. In *The electrochemistry of sulphide minerals. Trends in electrochemistry* edited by J.O'M. Bockris, D.A.J. Rand and B.J. Welch, Plenum Press, New York, 1976, p. 267.

3. NATARAJAN , K.A., RIEMER, S.C., IWASAKI, I. AND REID, K.J. Electroleaching of a Dulth gabro copper-nickel concentrate. Part I: Electrochemical studies on selective nickel dissolution. Paper submitted for *XV Int. Miner. processing Congr.*,. Cannes, June 2–9, 1985.

4. NATARAJAN, K.A.. AND IWASAKI, I. Eh-pH response of noble metals and sulphide mineral electrodes, *Soc. Min. Engrs, AIME*, 1972, **252**, 437.

Thesis Abstract (M.Sc. Engng)

Some studies on reinforced concrete beam-column joints by A. Kumar.
Research supervisor: Prakash Desayi.
Department: Civil Engineering.

1. Introduction

This thesis deals with beam-column joints that are encountered in reinforced concrete-framed structures. The work presented consists of an experimental study of joint strength, deformations and crackwidths and a theoretical study of joint ultimate strength. As joints are the links between beams and columns of a frame, the study of their strength and performance is important.

Existing literature on the subject reveals that the strength of the joint is greatly affected by the manner in which reinforcement is detailed at the joint. Nilsson[1] found that joint specimens containing some of the commonly used reinforcement details developed a brittle failure within the joint at loads as low as 30% of the theoretical ultimate loads of the connecting members. The joint was weakend by the formation of a crack running diagonally across the joint which finally caused the failure. However, when reinforcements were so detailed as to cut across this potential failure crack, the joints developed higher strength[1,2]. Some of the problems requiring further research in the area of joints have been reported by an ACI-ASCE Committee[3].

2. Experimental work

After a detailed review of existing literature, an experimental programme was planned and carried out. It consisted of casting joint specimens and testing them under static, one-way loading. Three types of joints were tested *viz.*, the Opening L-joint (27 specimens), Closing L-joint (5 specimens) and T-joint (7 specimens). The aim of the testing was two fold: (i) to re-examine the behaviour and strength of some of the joint details studied by others and (ii) to propose/study alternative joint details which are easy to fabricate and have higher joint strength.

In the opening L-joints and T-joints, in addition to the above two, a third aspect was also investigated, *viz.*, (iii) strength and behaviour of joints with the beam being wider than column.

3. Test results

The specimens were loaded so as to produce maximum moments in the members at the joint faces. The failure observed in all the three types of joints was due to the diagonal crack linking the corners where the member flexural compressions were acting.

Defining the joint efficiency as the ratio of bending moment at the joint face at failure to the theoretical ultimate moment of the beam, out of the various details proposed in this study, those which were found to be the most efficient in specimens with beam and column of equal width are given in fig. 1 and Table I.

In beam-wider-than column joints vertical stirrup detail was used. The efficiencies of

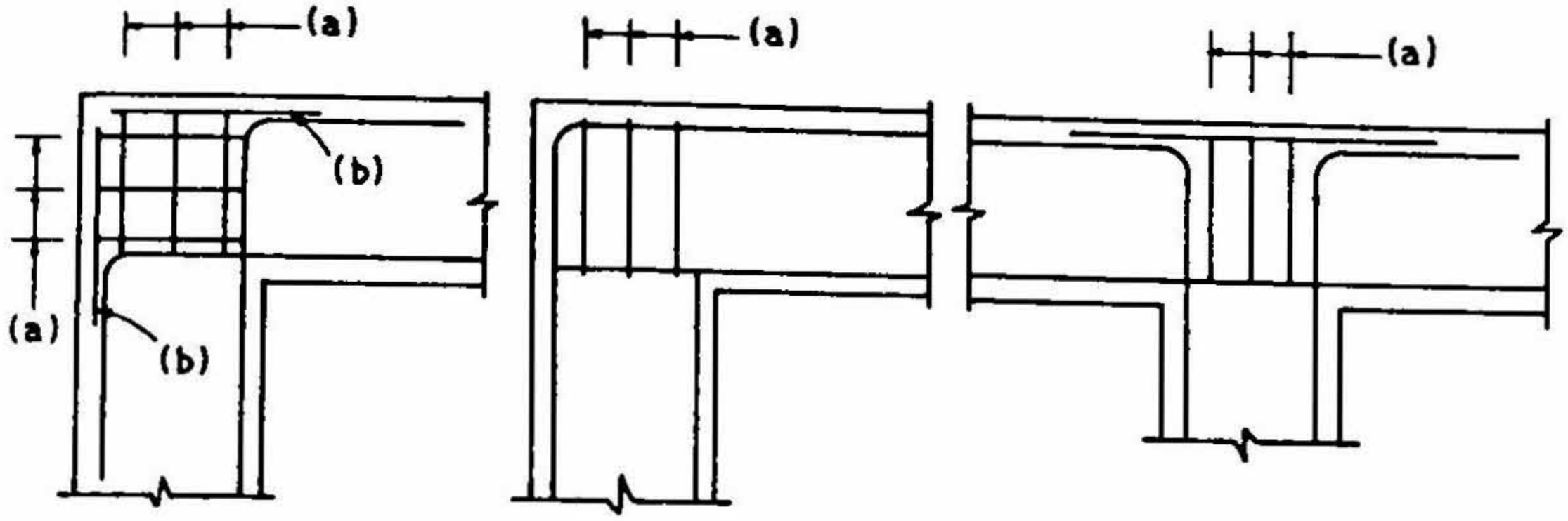

FIG. 1. Details of joints found most efficient in this study.
(a) 3 nos. two legged stirrups of 4 mm Ø bar.
(b) 2 nos. 6 mm Ø hanger bars.

these ranged from 48% to 90% in specimens with beam concentric with column and from 77% to 85% with beam eccentric with column.

Maximum crackwidth at working load was below 0.3 mm in all closing L-joint specimens, while in the opening L-joint and T-joint specimens, in all but one specimen, it exceeded 0.3 mm.

4. Theoretical analysis

A method, based on splitting of an assumed concrete cylinder at the joint, has been proposed for determining the joint strength. Figure 2 shows this model for the opening L-joint and it has been similarly extended for the other two joint types. Referring to fig.2, forces C_1-C_1 produce splitting tensile stress f_{t1} and forces C_2-C_2 produce a direct tensile stress f_{t2}. The failure takes place when $f_{t1} + f_{t2}$ equals the cylinder splitting tensile strength f_{sp} of concrete. The ultimate moment is determined as the product of the member flexural force (causing the splitting failure) and the internal lever arm in the member. Any reinforcement of area A_j which crosses the splitting plane is assumed to yield (stress f_{yj}) at

Table I
Details of joints and their efficiencies

Type of joint	Joint detail	Joint efficiency (%)
Opening L-joint	Stirrups in the horizontal and vertical directions	102
Closing L-joint	Stirrups in the vertical direction	87
T–joint	Stirrups in the vertical direction	138

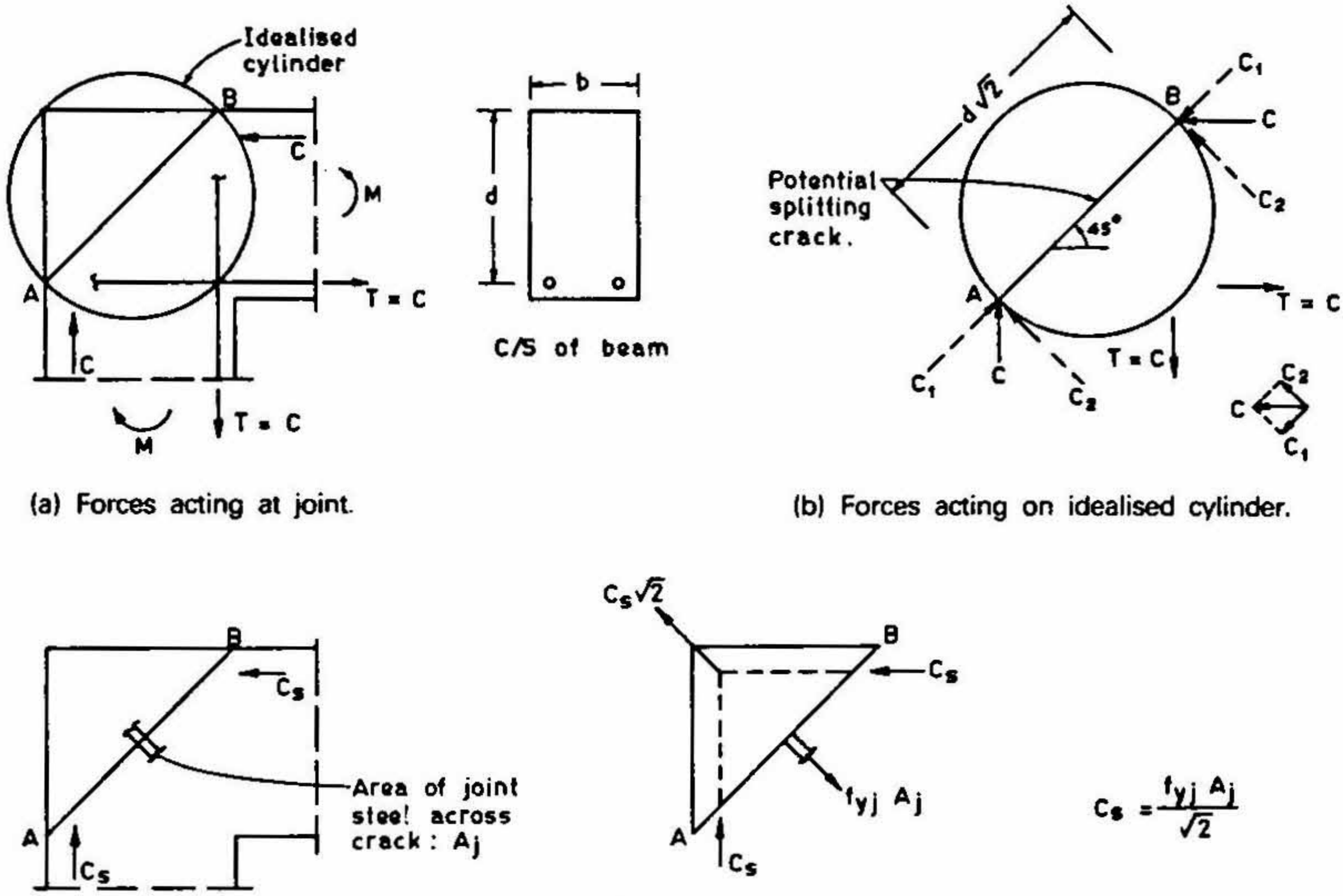

(a) Forces acting at joint. (b) Forces acting on idealised cylinder.

(c) Additional contribution of joint steel (C_s).

$$C_s = \frac{f_{yj} A_j}{\sqrt{2}}$$

FIG. 2. Analysis of opening L-joint at failure.

joint failure and its contribution added to that of concrete. Table II gives the expressions developed and the average ratio of computed to experimental ultimate moments (M_{uc}/M_{ue}) for the joints studied.

5. Conclusions

1. In opening L-joints and T-joints, the provision of stirrups in the joint, either in the vertical direction or in both horizontal and vertical directions, improves joint efficiency.

Table II
Ultimate moment at failure

Type of joint	Expression for M_{uc}	M_{uc}/M_{ue} (per cent)
Opening L-joint	$M_{uc} = 0{\cdot}607 f_{sp} bd^2 + 0{\cdot}566 f_{yj} A_j d$	86·6
Closing L-joint	$M_{uc} = 1{\cdot}256 f_{sp} bd^2 + 0{\cdot}566 f_{yj} A_j d$	97·2
T-joint	$M_{uc} = 0{\cdot}839 f_{sp} bd^2 + 0{\cdot}377 f_{yj} A_j d$	93·2

2. In closing L-joints, the simple detail with a 90° bend of the member reinforcement at the outer corner develops the full member strength.

3. In the beam-wider-than column joints, within the ranges studied, joint efficiency is not affected by beam eccentricity. Also, the anchorage strength of the beam tension bars is not affected by placing them outside the cage of column bars at the joint.

4. The proposed analysis has predicted, on an average, the ultimate strength of the joint satisfactorily and errs on the safer side.

References

1. NILSSON, I.H.E. AND LOSBERG, A. — Reinforced concrete corners and joints subjected to bending moment, *J. Struct. Div., Proc. Am. Soc. of Civ. Engrs.*, 1976, **102**(ST6), 1229–1254.

2. MAYFIELD, B., KONG, F.K. AND BENNISON, A. — Strength and stiffness of lightweight concrete corners, *J. Am. Concr. Inst.* 1972, **69**(7), 420–427.

3. ACI-ASCE Committee 352 — Recommendations for design of beamcolumn joints in monolithic reinforced concrete structures, *J. Am. Concr. Inst.*, 1976, **73**(7), 375–393.